Bi-allelic variants in neuronal cell adhesion molecule cause a neurodevelopmental disorder characterized by developmental delay, hypotonia, neuropathy/spasticity

Authors

Alina Kurolap, Florian Kreuder, Claudia Gonzaga-Jauregui, ..., Michael C. Kruer, Jan Kaslin, Hagit Baris Feldman

Correspondence

hagitbf@tlvmc.gov.il

Kurolap et al., 2022, The American Journal of Human Genetics *109*, 518–532
March 3, 2022 © 2022 American Society of Human Genetics.
https://doi.org/10.1016/j.ajhg.2022.01.004

CellPress

ARTICLE

Bi-allelic variants in neuronal cell adhesion molecule cause a neurodevelopmental disorder characterized by developmental delay, hypotonia, neuropathy/spasticity

Alina Kurolap,[1,2,3,28] Florian Kreuder,[4,28] Claudia Gonzaga-Jauregui,[5] Morasha Plesser Duvdevani,[6,7] Tamar Harel,[6,7] Luna Tammer,[8] Baozhong Xin,[9] Somayeh Bakhtiari,[10,11] James Rice,[12] Clare L. van Eyk,[12] Jozef Gecz,[12,13] Jean K. Mah,[14] Derek Atkinson,[15,16] Heidi Cope,[17] Jennifer A. Sullivan,[17] Alon M. Douek,[4] Daniel Colquhoun,[4] Jason Henry,[18] Donald Wlodkowic,[18] Yesim Parman,[19] Ayşe Candayan,[20] Elif Kocasoy-Orhan,[21] Anat Ilivitzki,[3,21] Shiri Soudry,[3,22] Rina Leibu,[22] Fabian Glaser,[23] Valerie Sency,[9] Undiagnosed Diseases Network, Gil Ast,[8] Vandana Shashi,[17] Michael C. Fahey,[24] Esra Battaloğlu,[20] Albena Jordanova,[16,25] Vardiella Meiner,[6,7] A. Micheil Innes,[14,26] Heng Wang,[9] Orly Elpeleg,[6,7] Michael C. Kruer,[10,11] Jan Kaslin,[4,29] and Hagit Baris Feldman[1,2,3,27,29,*]

Summary

Cell adhesion molecules are membrane-bound proteins predominantly expressed in the central nervous system along principal axonal pathways with key roles in nervous system development, neural cell differentiation and migration, axonal growth and guidance, myelination, and synapse formation. Here, we describe ten affected individuals with bi-allelic variants in the neuronal cell adhesion molecule *NRCAM* that lead to a neurodevelopmental syndrome of varying severity; the individuals are from eight families. This syndrome is characterized by developmental delay/intellectual disability, hypotonia, peripheral neuropathy, and/or spasticity. Computational analyses of *NRCAM* variants, many of which cluster in the third fibronectin type III (Fn-III) domain, strongly suggest a deleterious effect on NRCAM structure and function, including possible disruption of its interactions with other proteins. These findings are corroborated by previous *in vitro* studies of murine *Nrcam*-deficient cells, revealing abnormal neurite outgrowth, synaptogenesis, and formation of nodes of Ranvier on myelinated axons. Our studies on zebrafish *nrcama*$^{\Delta}$ mutants lacking the third Fn-III domain revealed that mutant larvae displayed significantly altered swimming behavior compared to wild-type larvae ($p < 0.03$). Moreover, *nrcama*$^{\Delta}$ mutants displayed a trend toward increased amounts of α-tubulin fibers in the dorsal telencephalon, demonstrating an alteration in white matter tracts and projections. Taken together, our study provides evidence that *NRCAM* disruption causes a variable form of a neurodevelopmental disorder and broadens the knowledge on the growing role of the cell adhesion molecule family in the nervous system.

Introduction

Cell adhesion molecules (CAMs) are membrane-bound proteins that have an important role in tissue morphogenesis and maintenance. CAMs sustain an essential platform for intercellular signaling by mediating interactions between neighboring cells or between cells and the extracellular matrix.[1,2] In the central nervous system (CNS), the L1 subgroup of immunoglobulin (Ig)-CAMs is the most abundant, consisting of four structurally related proteins:

[1]The Genetics Institute and Genomics Center, Tel Aviv Sourasky Medical Center, Tel Aviv 6423906, Israel; [2]The Genetics Institute, Rambam Health Care Campus, Haifa 3525408, Israel; [3]Ruth and Bruce Rappaport Faculty of Medicine, Technion – Israel Institute of Technology, Haifa 3525428, Israel; [4]Australian Regenerative Medicine Institute, Monash University, Melbourne, VIC 3800, Australia; [5]Regeneron Genetics Center, Regeneron Pharmaceuticals Inc., Tarrytown, NY 10591, USA; [6]Department of Genetics, Hadassah Medical Center, Jerusalem 91120, Israel; [7]Faculty of Medicine, Hebrew University of Jerusalem, Jerusalem 9112102, Israel; [8]Department of Human Molecular Genetics and Biochemistry, Sackler Faculty of Medicine, Tel Aviv University, Tel Aviv 6997801, Israel; [9]DDC Clinic - Center for Special Needs Children, Middlefield, OH 44062, USA; [10]Pediatric Movement Disorders Program, Division of Pediatric Neurology, Barrow Neurological Institute, Phoenix Children's Hospital, Phoenix, AZ 85013, USA; [11]Departments of Child Health, Neurology, and Cellular and Molecular Medicine, and Program in Genetics, University of Arizona College of Medicine - Phoenix, Phoenix, AZ 85004, USA; [12]Paediatric Rehabilitation, Women's and Children's Hospital, Adelaide, SA 5006, Australia; [13]South Australian Health and Medical Research Institute, Adelaide, SA 5000, Australia; [14]Department of Pediatrics and Alberta Children's Hospital Research Institute, Cumming School of Medicine, University of Calgary, Calgary, AB T2N 4N1, Canada; [15]Max Planck Institute of Immunobiology and Epigenetics, Freiburg 79108, Germany; [16]Molecular Neurogenomics Group, VIB-UAntwerp Center for Molecular Neurology, University of Antwerp, Antwerpen 2000, Belgium; [17]Division of Medical Genetics, Department of Pediatrics, Duke University Medical Center, Durham, NC 27710, USA; [18]School of Science, RMIT University, Melbourne, VIC 3000, Australia; [19]Department of Neurology, Istanbul Faculty of Medicine, Istanbul University, Istanbul 34093, Turkey; [20]Department of Molecular Biology and Genetics, Bogaziçi University, Istanbul 34342, Turkey; [21]Pediatric Radiology Unit, Rambam Health Care Campus, Haifa 3525408, Israel; [22]Department of Ophthalmology, Rambam Healthcare Campus, Haifa 3525408, Israel; [23]The Lorry I. Lokey Interdisciplinary Center for Life Sciences and Engineering, Technion – Israel Institute of Technology, Haifa 3200003, Israel; [24]Department of Pediatrics, Monash University, Melbourne, VIC 3800, Australia; [25]Molecular Medicine Center, Department of Medical Chemistry and Biochemistry, Medical University-Sofia, Sofia 1431, Bulgaria; [26]Department of Medical Genetics and Alberta Children's Hospital Research Institute, Cumming School of Medicine, University of Calgary, Calgary, AB T2N 4N1, Canada; [27]Sackler Faculty of Medicine, Tel Aviv University, Tel Aviv 6997801, Israel
[28]These authors contributed equally
[29]These authors contributed equally
*Correspondence: hagitbf@tlvmc.gov.il
https://doi.org/10.1016/j.ajhg.2022.01.004.
© 2022 American Society of Human Genetics.

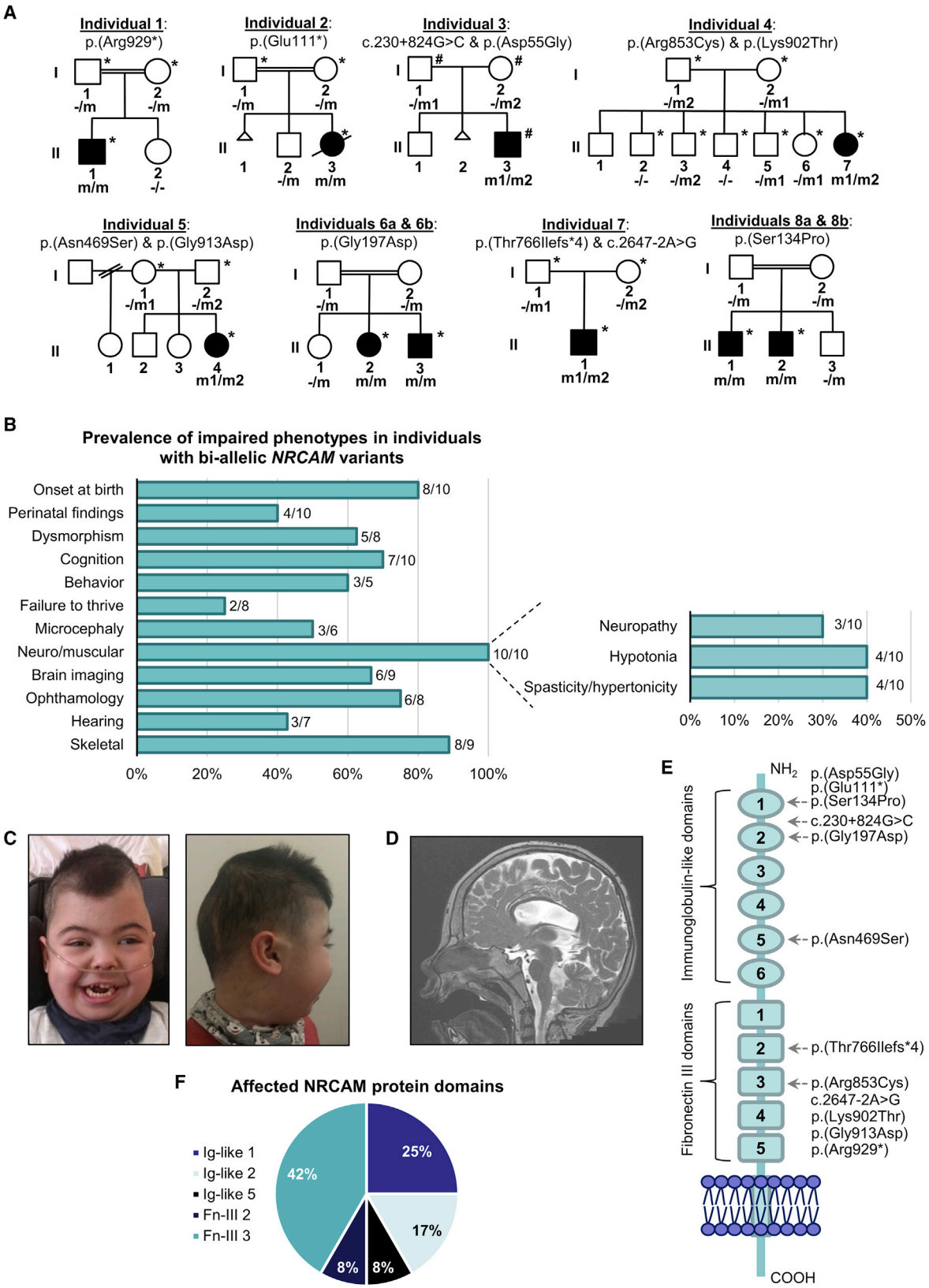

Figure 1. *NRCAM* variants in individuals with neurodevelopmental disease

(A) Pedigrees and variant segregation in eight families with ten affected individuals harboring bi-allelic *NRCAM* variants; individuals that underwent whole-exome sequencing (*) and whole-genome sequencing (#) are marked in each family.

(B) Frequency of phenotypic features in individuals with bi-allelic *NRCAM* variants.

(legend continued on next page)

L1CAM, NRCAM, CHL1, and neurofascin (NFASC). These proteins are predominantly expressed along principal axonal pathways, such as the corpus callosum, corticospinal tract, and the optic nerve.[3] L1-IgCAMs have been shown to serve several overlapping, as well as distinct, functions critical for nervous system development, including neural cell differentiation and migration, axonal growth and guidance, myelination, and synapse formation.[2–4] To date, variants in *L1CAM* (MIM: 308840) have been implicated in the most common cause for X-linked congenital syndromic and non-syndromic hydrocephalus, as well as several non-hydrocephalus phenotypes characterized by spastic paraplegia (MIM: 304100, 303350, 307000).[5,6] Bi-allelic variants in *NFASC* (MIM: 609145) have also been described in a neurodevelopmental disorder with central and peripheral motor dysfunction (MIM: 618356).[7–9]

In this study, we describe ten affected individuals with bi-allelic deleterious variants in *NRCAM* (MIM: 601581) that lead to a neurodevelopmental syndrome of varying severity, characterized by developmental delay, hypotonia, and peripheral neuropathy or spasticity; the individuals are from eight families. Furthermore, we show that zebrafish *nrcama*$^{\Delta}$ mutants display abnormal behavior and a trend toward disrupted axonal projections.

Subjects and methods

Participants and ethics

The study was approved by the institutional review boards of all participating institutions, and written informed consent was obtained from affected individuals or their caregivers. Participants were comprehensively examined by their treating neurologists and medical geneticists, and medical records were reviewed for additional data. We used the GeneMatcher platform to identify similar affected individuals worldwide.[10]

Genetic analysis

Whole-exome sequencing (WES) or whole-genome sequencing (WGS) was performed on Illumina-based platforms, as described previously (sequenced family members are indicated in Figure 1A);[11–14] for individuals 1 and 4, WES was performed in collaboration with the Regeneron Genetics Center.

Data analysis pipelines used were based on each pedigree, e.g., presence of consanguinity and number of affected individuals in the family. Briefly, WES/WGS data were filtered for the following: (1) rare variants (minor allele frequency [MAF] < 0.01 in healthy controls from the general population and in-house databases); (2) effect on protein product (missense, nonsense, frameshift, and splice-site variants); (2) different inheritance models, with emphasis on recessive inheritance due to parental consanguinity and/or multiple affected siblings in most families; and (4) proteins with function related to the CNS. Candidate variants were validated with Sanger sequencing. Segregation analyses were performed on the basis of the family pedigrees.

Variant analysis and protein structural modeling

To assess the pathogenicity of missense variants, we used the algorithms embedded in the Alamut Visual platform v2.10 (Interactive Biosoftware, Rouen, France). We used the Human Splicing Finder (HSF) tool to predict the consequence of intronic variants.[15] In addition, structural homology-based models of each affected NRCAM domain were built with the SWISS-MODEL server and validated for quality by the ProSA-web server.[16,17] This enabled us to review the structure of the mutated region and investigate the location and characteristics of the mutation sites. Surface electrostatics analysis was performed by the adaptive Poisson-Boltzmann solver (APBS),[18] and areas of potential protein-protein interactions were computed by optimal docking area (ODA) analysis, which provides interface prediction from protein surface desolvation energy.[19] UCSF Chimera software v1.13.1 was used for visualization.

Zebrafish studies

Fish were housed and bred within the Monash AquaCore Facility according to standard housing conditions under breeding license ERM14481. The *nrcama*$^{\Delta}$ zebrafish mutant was generated under ethics application ERM23532. Experiments were assessed and approved by the Monash University Animal Ethics Committee and were conducted under applicable Australian laws governing the care and use of animals for scientific research.

CRISPR-Cas9 mutagenesis of nrcama in zebrafish

The zebrafish *nrcama* gene (Zebrafish Information Network, ZFIN: ZDB-GENE-041210-235) is the sole ortholog of human *NRCAM*; there is 62.9% amino acid similarity between the zebrafish and human proteins. Another possible ortholog, *nrcamb*, was proposed on the basis of older genome builds (ZFIN: ZDB-GENE-040426-1542); however, BLAST sequence analysis of the gene in a newer genome assembly (Ensembl GRCz11, ENSDARG00000006396) partially maps it to *cntn1a*. Furthermore, synteny analysis of *NRCAM* in the vertebrate lineage does not suggest duplication at this locus in zebrafish or loss of a second copy (Genomicus V93.01, V100.01).

For CRISPR-Cas9 mutagenesis, Alt-R CRISPR RNA (crRNA) guides, targeting sequences in exons 18 and 19 and to mutate or delete the third fibronectin type III (Fn-III) domain repeat, were designed with Integrated DNA Technologies online software (IDT, Newark, NJ, USA) (Table S1, Figure S1). We made gRNAs by annealing crRNAs to ATTO-555-conjugated *trans*-activating CRISPR RNAs (tracrRNAs). Active ribonucleoprotein (RNP) mix, comprised of Alt-R S.p. Cas9 V3 protein (IDT) in complex with *nrcama*-targeting gRNAs, was injected into the cytoplasm of 1-cell stage embryos. Embryos were then sorted for fluorescence of the tracrRNA.[20] Fluorescent embryos were used for further experiments and confirmation of targeted mutagenesis by PCR

(C) Facial dysmorphism of individual 1, including bi-temporal narrowing, bushy eyebrows with medial flaring, long eyelashes, depressed nasal bridge, and cupid bowed lips (left) and plagiocephaly (right).
(D) Sagittal T2W imaging of individual 1's brain reveals enlarged third and fourth ventricles and a thinned corpus callosum. The vermis is partially shifted off the midline yet not reduced in size.
(E) Schematic representation of the NRCAM protein domains. The location of variants observed in individuals with NRCAM-related disease are highlighted.
(F) Distribution of *NRCAM* variants among protein domains reveals a variant cluster in the third Fn-III domain repeat.

screening of larval gDNA (Figures S1B and S1C). A germline *nrcama* mutant with a 302 base-pair deletion of large parts of exon 18 and 19 was identified and characterized (*nrcama*$^{\Delta}$). This deletion results in a frameshift and premature stop codon toward the end of the residual exon 19 fragment (Figures S1D–S1F).

Immunohistochemistry

Zebrafish embryos and larvae were fixed in 4% paraformaldehyde diluted in phosphate buffer (pH 7.4); brains were dissected and processed for immunohistochemistry, as previously described.[21] Primary antibodies included anti-double phosphorylated-extracellular signal-regulated kinase (dp-ERK, #9101, Cell Signaling Technologies, Danvers, MA, USA), anti-serotonin (5-HT, S5545, Sigma-Aldrich, St. Louis, MO, USA), and anti-α-tubulin (T6199, Sigma-Aldrich), as previously used in zebrafish.[22,23] For details see supplemental methods.

Confocal fluorescent images were acquired via a Leica TCS SP5 or SP8 confocal microscope (Leica Microsystems, Wetzlar, Germany); brightness and contrast were adjusted with FIJI/ImageJ or LAS AF Lite software.

Behavioral assays and analysis

We performed all experiments on progeny derived from F1 heterozygous in-crosses to remove any cohort bias, as wild-type, heterozygous, and homozygous mutant siblings were sampled randomly. All experiments were blind because genotyping was performed as the final step of the analysis pipeline. Acquisition of behavioral data was performed with a custom-built digital video imaging system (see supplemental methods). Behavioral assays were performed in larvae at 5 days post fertilization (dpf). Larvae were placed in a custom plastic plate made up of 18 individual circular chambers (15.6 mm in diameter, 3 mm deep). Animals were initially acclimatized for 2 min prior to video recording of the baseline locomotion. Baseline locomotion assays were performed on acclimatized fish in white light or in complete darkness for 6 min. The acquired files were then analyzed with an animal tracking software Ethovision XT v.15 (Noldus Information Technology, Wageningen, the Netherlands); average distance traveled, average speed, and time in zone center of arena were quantified.

Quantification and statistical analysis

GraphPad Prism 9 (GraphPad Software, San Diego, CA, USA) was used for all statistical analyses and graph construction. We used the Shapiro-Wilk normality test to confirm data adhered to a Gaussian distribution, and we performed log transformation if data was found to be lognormal. We used unpaired t tests (two-tailed) to compare differences between two groups. For all experiments, significance was accepted at $p < 0.05$. All statistical results, including exact p values, are reported in figure legends. Graphical data represent mean ± standard deviation.

Results

Phenotype and genotype of NRCAM-related disease

Clinical evaluation

Through international collaboration, we identified ten affected individuals (Figure 1A), all presenting with neurodevelopmental findings of varying severity; the individuals are from eight families. The phenotypic manifestations are summarized in Table 1 and Figure 1B, and detailed case reports are available in the supplemental notes.

All affected individuals, excluding the proband of family 7 and the brothers of family 8, presented with global developmental delay (GDD) and cognitive impairment, combined with either hypotonia and neuropathy or spasticity. Individuals 1 and 2 were the most severely affected, including hydrocephalus, GDD, failure to thrive, hypotonia, and neuropathy in individual 1 and an early demise of individual 2 at 21 months. Figures 1C and 1D shows individual 1's dysmorphic features and brain imaging. Individuals 3–6 presented with facial dysmorphism, GDD, intellectual disability, hypotonia, ataxia, peripheral neuropathy or spasticity, and visual and hearing abnormalities with variable penetrance. Individual 7 presented with a severe phenotype at birth, resembling that of individual 1, but most of his neuromuscular symptoms improved over time and he exhibits no signs of intellectual disability at age 5 years. Individuals 8a and 8b exhibit the mildest phenotype; both presented with late-onset peripheral neuropathy without developmental delay.

Of note, individual 1 has a concomitant homozygous loss-of-function (LoF) variant in *CD55* (MIM: 125240), causing protein-losing enteropathy (PLE) and hypercoagulopathy (MIM: 226300), as previously reported.[24] Shortly after PLE onset, he suffered from seizures attributed to sinus vein thrombosis secondary to the CD55 loss, which resolved on treatment with eculizumab.[25] Additionally, individual 3 has a mosaic (10%–20%) likely pathogenic variant in *KRAS* (c.355G>A [p.Asp119Asn]) (MIM: 190070) identified by clinical WES. Prior functional studies have indicated that this variant exerts a dominant-negative effect and individuals would be expected to have some symptoms associated with a RASopathy (MIM: 609942, 614470).[26,27] However, this variant did not explain his full clinical presentation, prompting research-based WGS.

Genetic analysis

We did not observe any candidate variants in known neurodevelopmental disease-causing genes on WES (individuals 1, 2, and 4–8) and WGS (individual 3) analyses. Further investigation by filtering criteria described above yielded bi-allelic *NRCAM* (GenBank: NM_001037132.2) variants for each of the affected individuals; details on genotype, allele frequency, amino acid conservation, and pathogenicity predictions are summarized in Table 2.

The deep intronic variant observed in individual 3 (c.230+824G>C) is predicted to disrupt a site for the splicing regulator SC35, which is required for spliceosome assembly and splice-site selection.[28] HSF software predicts that c.230+824G>C may cause activation of a cryptic acceptor site leading to generation of a cryptic exon.

Because *NRCAM* encodes a neuronal cell adhesion molecule involved in neural development, it was prioritized as the leading candidate for the neurological phenotypes observed. All *NRCAM* variants co-segregated with the disease in each family as expected on the basis of the pedigrees (Figure 1A).

In silico analysis of missense variants

All missense variants were predicted to be deleterious to protein function by at least two out of three

Table 1. Clinical manifestations of *NRCAM*-related neurodevelopmental disease

	Individual 1	Individual 2	Individual 3	Individual 4	Individual 5	Individual 6a	Individual 6b	Individual 7	Individual 8a	Individual 8b
Gender	M	F	M	F	F	F	M	M	M	M
Current age	5 years	21 months (deceased)	24 years	8 years	14 years	41 years	31 years	5 years	31 years	27 years
Country	Israel	Israel	USA	USA	Australia	Israel	Israel	Canada	Turkey	Turkey
Ancestry	Muslim Arab	Muslim Arab	European/ Chinese	Amish	European	Libyan Jewish	Libyan Jewish	European/ Asian/North American	Turkish	Turkish
Variant 1	c.2785C>T (p.Arg929*)	c.331G>T (p.Glu111*)	c.164A>G (p.Asp55Gly)	c.2557C>T (p.Arg853Cys)	c.1406A>G (p.Asn469Ser)	c.590G>A (p.Gly197Asp)	c.590G>A (p.Gly197Asp)	c.2297_ 2302delinsTC (p.Thr766Ilefs*4)	c.400T>C (p.Ser134Pro)	c.400T>C (p.Ser134Pro)
Variant 2	c.2785C>T (p.Arg929*)	c.331G>T (p.Glu111*)	c.230+824G>C	c.2705A>C (p.Lys902Thr)	c.2738G>A (p.Gly913Asp)	c.590G>A (p.Gly197Asp)	c.590G>A (p.Gly197Asp)	c.2647−2A>G	c.400T>C (p.Ser134Pro)	c.400T>C (p.Ser134Pro)
Clinical characteristics										
Onset	birth	birth	birth	birth	birth	birth	birth	birth	20 years	15 years
Perinatal findings	polyhydramnios	IUGR	none	none	premature membrane rupture	none	none	polyhydramnios	none	none
Dysmorphism	bi-temporal narrowing, plagiocephaly, bushy eyebrows with medial flaring, long eyelashes, depressed nasal bridge, cupid bowed lips, micrognathia	round facies, infra-lateral periorbital fullness, mild synophrys, deeply grooved philtrum, tented mouth, vaulted palate, micrognathia	coarse facies, bushy eyebrows, elongated face, hypertelorism, upslanting palpebral fissures, flat nasal bridge, small nose, micrognathia	tented upper lip and prominent cheeks	none	N/A	N/A	mildly hypotonic facies, posteriorly rotated ears, small chin, high arched palate	none	none
Developmental delay	severe GDD	severe GDD	severe ID, ASD	GDD	GDD	ID, motor delay	ID, motor delay	gross and fine motor delays (improved)	none	none
Behavioral issues	self-injurious behavior	N/A	irritability, self-injurious behavior	anxiety, irritability, and aggression	N/A	N/A	N/A	N/A	normal	normal
Growth parameters	weight −2.4 SD; height −2.5 SD.	normal	weight −2.32 SD; height −2.75 SD.	normal	normal weight	N/A	N/A	normal	normal	normal
Head circumference	microcephaly (−3.5 SD)	microcephaly (−2.6 SD)	microcephaly (−3.09 SD)	normal	N/A	N/A	N/A	normal	N/A	N/A

(*Continued on next page*)

Table 1. ***Continued***

	Individual 1	Individual 2	Individual 3	Individual 4	Individual 5	Individual 6a	Individual 6b	Individual 7	Individual 8a	Individual 8b
Neurological and neuromuscular	axial hypotonia, mild motor-sensory demyelinating polyneuropathy	axial and peripheral hypotonia, decreased deep tendon reflexes, laryngomalacia	hypertonia of all extremities, decreased muscle bulk, ataxia, abnormal EEG w/o apparent seizures	hypotonia, ataxia	severe hypertonia, spastic quadriplegic CP, prominent jaw jerk	spastic-dystonic paraplegic CP	spastic-dystonic paraplegic CP, epilepsy at 5 years	distal arthrogryposis (improved), axial hypotonia, non-specific myopathy, tracheomalacia, vocal cord paralysis (improved)	motor neuropathy with secondary myopathic involvement	motor neuropathy with secondary myopathic involvement
Brain imaging	hydrocephalus, thin corpus callosum, partially shifted vermis	normal	bil PVL, partially empty sella, subependymal nodular gray matter heterotopia, bil hypo-/delayed myelination, hypoplastic pituitary gland	normal	bil PVL with reduced white matter volume, thinned corpus callosum and elements of delayed myelination	ventriculomegaly, colpocephaly, elongation of the left Sylvian fissure to the periventricular white matter	mild ventriculomegaly	normal	arachnoid cyst of the posterior fossa	N/A
Ophthalmology	optic atrophy, abnormal VEP, exotropia	mild hyperopia	bil retinal detachment, cataract	mild myopia with astigmatism, optic cupping	strabismus with accommodative/alternating esotropia	N/A	N/A	normal	cataract	normal
Hearing	abnormal BERA	mild hearing loss	N/A	abnormal BERA	normal	N/A	N/A	normal	normal	normal
Skeletal findings	congenital hip dysplasia, severe scoliosis, pes cavus, tapering fingers	N/A	severe scoliosis, left acetabulum dysplasia, bil hip dysplasia, bil coxa valga, pes planus	pes planus	hip dysplasia, subluxing hips	none	scoliosis	bil hip dislocation	severe scoliosis, pes cavus, hammer toes	severe scoliosis, pes cavus, hammer toes
Other features and co-morbidities	oxygen supplementation, gastrostomy feeding, cryptorchidism, CD55-deficiency	oxygen supplementation, gastrostomy feeding, severe GERD	bil cryptorchidism, two large hypopigmented macules, mosaic *KRAS* variant	none	none	precocious puberty, leukemia at 3 years	none	oxygen supplementation and tracheostomy (resolved), cryptorchidism, gastrostomy feeding (improved), constipation	CPKemia	CPKemia

Abbreviations: ASD, autism spectrum disorder; BERA, brain-stem-evoked response auditory; bil, bilateral; CP, cerebral palsy; CPK, creatine phosphokinase; EEG, electroencephalogram; F, female; GERD, gastresophageal reflux disease; GDD, global developmental delay; ID, intellectual disability; IUGR, intrauterine growth restriction; M, male; N/A, not available; PVL, periventricular leukomalacia; SD, standard deviations; VEPs, visual-evoked potentials; w/o, without.

Table 2. Bi-allelic *NRCAM* (GenBank: NM_001037132.2) variants observed in affected individuals

	Individual 1	Individual 2	Individual 3		Individual 4		Individual 5		Individuals 6a and 6b	Individual 7		Individuals 8a and 8b
cDNA effect	c.2785C>T	c.331G>T	c.164A>G	c.230+824G>C	c.2557C>T	c.2705A>C	c.1406A>G	c.2738G>A	c.590G>A	c.2297_2302delinsTC	c.2647−2A>G	c.400T>C
Protein effect	p.Arg929*	p.Glu111*	p.Asp55Gly	N/A	p.Arg853Cys	p.Lys902Thr	p.Asn469Ser	p.Gly913Asp	p.Gly197Asp	p.Thr766Ilefs*4	N/A	p.Ser134Pro
Zygosity	hom	hom	comp het	comp het	comp het	comp het	comp het	comp het	hom	comp het	comp het	hom
Exon	25	7	6	intron 6	24	25	15	25	9	22	intron 24	7
Protein domain	Fn-III 3	Ig-like 1	Ig-like 1	Ig-like 1-2	Fn-III 3	Fn-III 3	Ig-like 5	Fn-III 3	Ig-like 2	Fn-III 2	Fn-III 3	Ig-like 1
dbSNP	–	–	rs1413634373	rs575851831	rs150373689	rs139634064	rs201033539	–	rs772993703	–	rs1298979445	–
1000 Genomes	–	–	–	–	0.026%	0.026%	0.026%	–	–	–	–	–
gnomAD	–	–	0.0004%	0.032%	0.023%	0.032%	0.022%	–	0.002%	–	–	–
GERP	5.56	5.28	5.61	–	5.36	5.55	5.2	4.61	5.55	–	–	4.9
CADD	43	37	25.4	–	26.2	25.4	22.5	26.5	26.4	–	–	25.2
SIFT	–	–	deleterious	–	deleterious	deleterious	deleterious	deleterious	deleterious	–	–	deleterious
PolyPhen-2	–	–	benign	–	probably damaging	possibly damaging	benign	probably damaging	probably damaging	–	–	probably damaging
MutationTaster	disease causing	disease causing	disease causing	–	disease causing	disease causing	disease causing	disease causing	disease causing	disease causing	disease causing	disease causing

Abbreviations: CADD, combined annotation-dependent depletion; comp het, compound heterozygous; Fn-III, fibronectin type III; GERP, genomic evolutionary rate profiling; hom, homozygous; Ig, immunoglobulin; NHLBI-ESP, NHLBI Exome Sequencing Project.

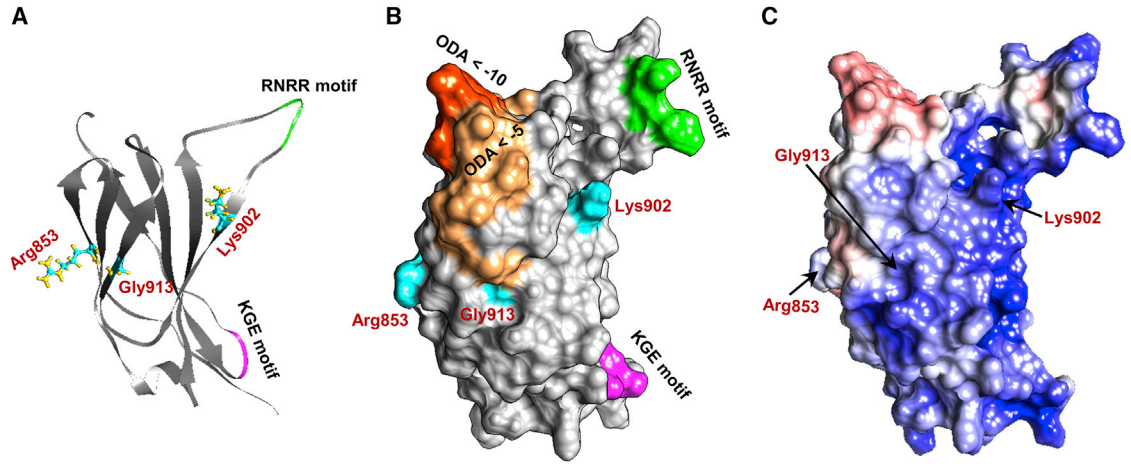

Figure 2. Structural modeling of the NRCAM third fibronectin type III (Fn-III) domain repeat

The third Fn-III domain repeat contains a cluster of the variants identified in affected individuals, including three missense variants (p.Arg853Cys, p.Lys902Thr, and p.Gly913Asp) and two predicted loss-of-function variants (p.Arg929* and c.2647−2A>G). (A and B) Three-dimensional (3D) structure (A) and surface (B) of the Fn-III 3 domain. Residues involved in nonsynonymous changes—Arg853, Lys902, and Gly913—are depicted in cyan, and the domain's KGE (magenta) and RNRR (green) motifs are highlighted. Optimal docking area (ODA) computation revealed regions predicted to belong to a protein-protein interface (dark orange represents ODA < -10 and light orange represents regions with ODA < -5). All three mutated residues are located either within or very close to the predicted ODA. Residue Lys902 is also located close to the domain's KGE and RNRR motifs, which are important for protein-protein interactions.

(C) Surface electrostatics analysis shows a clear electrostatic separation between negatively charged (red) and positively charged (blue) regions. The ODA depicted in (B) corresponds to the positively charged patch.

commonly used algorithms (SIFT, PolyPhen-2, and MutationTaster) and are either moderately or highly conserved among species, as detailed in Table 2 and Figure S2.

The *NRCAM* gene comprises a total of 33 exons (30 protein-coding), which undergo alternative splicing to produce multiple isoforms.[29] The canonical protein transcript (GenBank: NM_001037132.2) encodes a protein of 1,304 amino acids. Consistent with other Ig-CAMs, NRCAM structure includes a large N-terminal extracellular region, which consists of six Ig-like domains followed by five Fn-III repeats, a transmembrane region, and an intracellular C terminus (Figure 1E).[4,29,30]

Based on the obtained structural models, all substituted amino acids (Asp55, Ser134, Gly197, Asn469, Arg853, Lys902, and Gly913) appear exposed to the solvent (Figures 2 and S2). Because most of the amino acid substitutions change the polarity and/or charge of the residues, they are predicted to affect the protein's electrostatic balance, thus possibly disrupting NRCAM function and interactions.

The third Fn-III domain, which contains a large positively charged patch as evidenced by surface electrostatics analysis, appears to be a hotspot for mutagenesis. Three missense variants and two LoF variants (nonsense and splice-site) are localized within this domain (Figures 1E and 2). The residues Arg853, Lys902, and Gly913 are located either very close to or within the positive patch (Figure 2C), such that removing a positive charge (p.Arg853Cys, p.Lys902Thr) or changing the amino acid polarity (p.Gly913Asp) will most likely impact domain function. Moreover, fibronectin sites of interaction with other molecules have previously been mapped to a short stretch of amino acids, such as the Arg-Gly-Asp (RGD) motif, which is most commonly recognized by integrin heterodimers.[3,31] Although only L1CAM has an inherent RGD sequence,[3] it appears that NRCAM contains an equivalent motif in its third Fn-III domain: Lys-Gly-Glu (KGE)[32] at positions 934–936, which may confer similar properties. In addition, the third Fn-III domain of NRCAM contains an internal furin protease recognition site (RNRR, residues 894–897), which is used for proteolytic processing of such proteins, and may play a role in the domain's affinity to other adhesion molecules.[3] The 3D structural analysis of the domain reveals that both KGE and RNRR motifs are located close to the Lys902Thr mutant position (Figure 2). Given this data, the p.Lys902Thr variant may impact NRCAM protein-protein interactions, which are specific for this domain.

Optimal docking area (ODA) analysis revealed an area potentially involved in NRCAM interactions; regions strongly predicted to belong to an interface have an ODA value below -10 and involve residues Phe921, Pro948, and Glu949, while regions with ODA < -5 may also be significant and involve residues Val857, Asn858, Thr860, Gln889, Met914, Pro920, Thr947, and Gly950 (Figure 2B). Interestingly, this area is positioned on a slightly negative patch (electrostatics analysis, Figure 2C), located almost exactly within the triangle between the three variant positions (Arg853, Lys902, and Gly913), and on the opposite site to the KGE and RNRR motifs (Figure 2B). These findings suggest a possible disruption

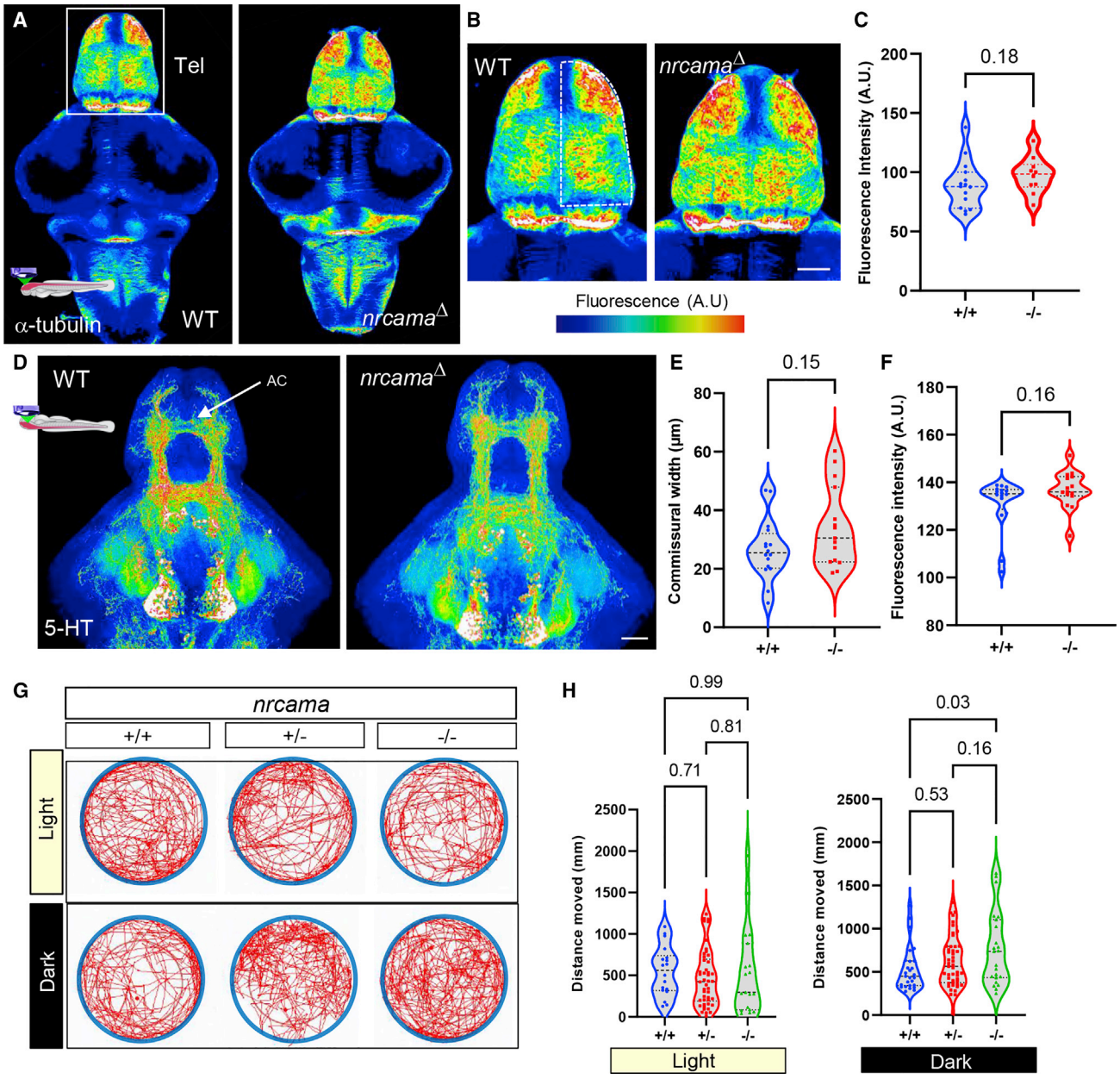

Figure 3. Zebrafish *nrcama*$^{\Delta}$ mutants display altered axonal projections and behavioral activity

(A and B) Confocal imaging and maximum intensity projection of whole-mount 5-day-old larval brain immunostained against α-tubulin, labeling axonal processes. The brains are imaged from the dorsal side and showing the telencephalon (Tel). Heatmap color scale to demonstrate regions with high fluorescence intensity (black, low intensity and red/white, high intensity).

(C) Quantification of fluorescence intensity (arbitrary units, A.U.) show *nrcama*$^{\Delta}$ mutant larvae display a trend toward an increased number of axons and terminals in the dorsal telencephalon (dashed outline in B) compared to wild-type siblings ($p = 0.18$; wild type 89.18 ± 19.95 A.U. $n = 15$; *nrcama*$^{\Delta}$ 97.50 ± 15.41 A.U., $n = 10$; variance shown as standard deviation from mean).

(D) 5-HT immunostaining of 5-day-old brain imaged from the ventral side, showing hypothalamic cell groups and ascending fiber projections, including the anterior telencephalic commissure (AC). Heatmap color scale to demonstrate regions with high fluorescence intensity (black, low intensity and red/white, high intensity).

(E and F) Quantification of fluorescence intensity (arbitrary units, A.U.) in the telencephalon shows a trend toward increased thickness of the anterior commissure ($p = 0.15$; wild type 26.6 ± 10.3 A.U., $n = 16$; *nrcama*$^{\Delta}$ 34.3 ± 13.8 A.U., $n = 15$; variance shown as standard deviation from mean), and mean intensity ($p = 0.16$; wild type 131.1 ± 10.9 A.U., $n = 16$; *nrcama*$^{\Delta}$ 136.8 ± 7.7 A.U., $n = 15$; variance shown as standard deviation from mean) in the *nrcama*$^{\Delta}$ mutant larvae compared to wild-type siblings.

(G) Overview of general locomotion in 5-day-old freely swimming *nrcama*$^{\Delta}$ mutants and wild-type siblings shown as average distance moved in mm during 6 min in white light or darkness. Swimming pattern and trajectory plotted as red line for each genotype in the arena (blue circle).

(H) Quantification of general locomotion in light or darkness. Under white light conditions, *nrcama*$^{\Delta}$ mutants and wild-type siblings displayed similar locomotion behavior ($p = 0.99$; wild type 550.3 ± 299.8 mm, $n = 18$; heterozygous *nrcama*$^{\Delta}$ 466.2 ± 345.1 mm, $n = 46$; homozygous *nrcama*$^{\Delta}$ 531.7 ± 526.9 mm, $n = 19$). However, mutants displayed significantly increased swimming activity in darkness ($p = 0.03$; wild type 530.3 ± 258.9 mm, $n = 27$; heterozygous *nrcama*$^{\Delta}$ 613.7 ± 295.7 mm, $n = 47$; homozygous *nrcama*$^{\Delta}$ 764.4 ± 428.2 mm, $n = 23$).

of interaction with another protein caused by the missense variants.

Altered neurodevelopment and behavior in mutant *nrcama*$^{\Delta}$ zebrafish

To functionally validate and elaborate on the role of *NRCAM* during neurodevelopment, we used zebrafish as an animal model. *NRCAM* has a direct zebrafish ortholog—*nrcama*—that is molecularly well conserved, including the Fn-III domains. To elaborate on the physiological significance of the third Fn-III domain repeat, which is a likely disease-causing hotspot that clusters most of the variants observed in the affected individuals, we used a CRISPR-Cas9 approach to mutate *nrcama* at the third Fn-III repeat in zebrafish (Figure S1). Microinjection of the *nrcama*-targeting gRNA-Cas9 complexes in zebrafish resulted in efficient ablation of the third Fn-III domain in zebrafish larvae (Figure S1). CRISPR-Cas9-injected and germline mutant *nrcama*$^{\Delta}$ embryos were viable and did not display gross morphological phenotypes impacting the body plane or the CNS. To visualize neuronal tracts and cell nuclei in the brain, we performed immunostaining of α-tubulin and serotonin (5-HT) in whole-mount brains of 5-day-old zebrafish larvae (Figures 3A–3F and S3). Mutant fish displayed a trend toward increased amounts of α-tubulin fibers in the dorsal telencephalon (Figures 3B and 3C), and a trend toward increased thickness of 5-HT-labeled ascending fiber tracts in the anterior telencephalic commissure was detected (Figures 3D–3F). These findings demonstrate some alteration in white matter tracts and projections in the presence of mutant *nrcama*$^{\Delta}$. To further elaborate on the findings and examine global neural cell function, we performed immunostainings of double phosphorylated-extracellular signal-regulated kinase (dp-ERK). ERK is phosphorylated upon neuronal activity and Ca^{2+} influx, and it can be used as a proxy marker for neurons and neuronal clusters displaying high levels of activity.[33] No significant change in number of dp-ERK positive cells or fluorescent intensity of cells was detected between wild-type siblings and *nrcama*$^{\Delta}$ mutant larval brains (Figures S3C and S3D).

To examine whether the alterations observed in telencephalic commissural axon density were accompanied by behavioral changes, we performed automated video tracking of general locomotion in freely swimming 5-day-old larvae. The mutant *nrcama*$^{\Delta}$ larvae did not display abnormal swimming behaviors compared to wild-type siblings under bright light (mimicking daylight) that stimulates swimming (Figure 3G), but a significant increase in swimming activity of the *nrcama*$^{\Delta}$ mutant was detected under darkness, when larvae are normally less active (Figures 3G and 3H).

Taken together, these experiments demonstrate that *nrcama*$^{\Delta}$ mutant zebrafish display minor alterations to axonal projections in the telencephalon and abnormal activity-driven behaviors in larvae.

Discussion

In this study, we describe ten affected individuals with bi-allelic variants in *NRCAM* presenting with a neurodevelopmental syndrome characterized mainly by GDD/intellectual disability, hypotonia, peripheral neuropathy, and/or spasticity, along with visual and hearing disturbances.

The neuronal cell adhesion molecule (NRCAM) is a member of the L1-Ig-CAM superfamily and, as such, has important roles in neural development.[30] NRCAM is predominantly expressed in the developing and mature nervous system in a pattern similar to L1CAM, including the floor plate and cerebellar granule cells, and both proteins have several overlapping functions.[34,35] Not coincidentally, the affected individuals described here share several clinical features with L1CAM-related disease, including GDD, hydrocephalus, and agenesis of the corpus callosum.[6] Another L1-Ig-CAM family member is neurofascin (NFASC), which is abundant in the cerebellum and peripheral nerves; *NFASC* bi-allelic variants have been described in three individuals presenting with a neurodevelopmental phenotype highly reminiscent of NRCAM-related disease, including GDD, hypotonia, peripheral neuropathy, or hypertonicity.[7–9] Similar to L1CAM- and NFASC-related disease, affected individuals with *NRCAM* bi-allelic variants exhibit a phenotypic spectrum, ranging from severe to mild disease.

Contrariwise to L1CAM, which is widely expressed throughout the brain, NRCAM expression is restricted mainly to neurons and glial cells in the ventral midline, e.g., spinal cord floor plate, optic chiasm, cerebellum, corpus callosum, and median eminence. In addition, high *Nrcam* expression levels have been observed in mice during motor neuron development, as well as in the neuromuscular junction and the inner ear.[3,30,36] These patterns correspond to the phenotypic features of the affected individuals described here, such as hydrocephalus, agenesis of corpus callosum, peripheral neuropathy, hypotonia, spasticity, ophthalmological abnormalities, and hearing loss (Table 1). Although it has not been previously described in the context of a monogenic disease, genetic association studies and animal behavioral analyses have linked NRCAM with several neuropsychiatric conditions in humans and mice, including autism, addiction susceptibility, schizophrenia, and behavioral abnormalities (e.g., impulsivity and fear conditioning),[30,37,38] and low NRCAM levels in cerebrospinal fluid has been suggested as a biomarker for early Alzheimer disease.[30] Accordingly, we observed significant behavioral changes in *nrcama*$^{\Delta}$ zebrafish mutants (Figures 3G and 3H), which displayed increased movement in darkness, suggesting an enhanced predatory response or exploratory boldness.[39] Behavioral studies in zebrafish have often been utilized to study the effects of different brain regions and neuropathology on behavior, and responses to light/dark conditions are used to study stress and anxiety responses and for evaluation

of neuroactive drugs for mood, anxiety, and sleep disorders.[40,41] While no alteration in sleep or night-time behavior has been noted in the individuals with bi-allelic *NRCAM* variants, other behavioral issues—most prominently aggression and self-injury—have been described in three individuals in our cohort (Figure 1B, Table 1). Long-term follow-up and additional affected individuals are required to determine whether other neuropsychiatric manifestations characterize individuals with bi-allelic *NRCAM* variants.

The extracellular region of NRCAM is composed of six Ig-like domains followed by five Fn-III domains and is critical for the protein's interaction with other CAMs and molecules enabling cell-cell interactions and adhesion.[1,4,30,42] The Ig-like domains are important for recognizing and binding ligand proteins and forming cell-cell interactions, while the Fn-III repeats mediate adhesion signaling through interactions with other proteins, such as integrins.[1,31,43] These interactions facilitate NRCAM's function in myelination, axonal growth and guidance, and synapse formation.[30] The p.Arg929*, p.Glu111*, and p.Thr766Ilefs*4 variants clearly lead to premature stop-codons, while the c.2647−2A>G splice variant is predicted to cause exon 22 skipping resulting in p.Ile883Serfs*8, thus truncating the protein product and impeding its function. The observed missense variants were found to affect either the Ig-like domains 1 (p.Ser134Pro), 2 (p.Gly197Asp), and 5 (p.Asn469Ser) or the third Fn-III domain (p.Arg853Cys, p.Lys902Thr, and p.Gly913Asp) (Figures 1D, 2, and S2). As noted by the *in silico* protein analyses, these variants are predicted to have an effect on protein function, most likely by abrogating its ability to interact with other proteins. The aggregation of most disease-causing variants in the third Fn-III domain repeat (Figures 1E and 2) highlights its importance for proper protein function.

Correspondingly, deletion of the third Fn-III domain repeat in zebrafish *nrcama* resulted in significantly altered swimming activity in the *nrcama*$^{\Delta}$ mutant fish (Figures 3G and 3H). Furthermore, homozygous mutant *nrcama*$^{\Delta}$ zebrafish larvae displayed a minor brain phenotype with a trend toward white matter tracts and axonal projections abnormalities within the dorsal telencephalon and a higher axonal density in the telencephalic anterior commissure (Figures 3A–3F). Consistent with this, the dorsal telencephalon has been identified as critical in the control of activity and fear responses.[44,45] Brain imaging of individuals with *NRCAM* mutations identified diverse morphological phenotypes, including a thin corpus callosum with partially shifted vermis, ventriculomegaly, periventricular leukomalacia, and delayed myelination, while some individuals had normal brain imaging (Figure 1D, Table 1). Interestingly, the dorsal telencephalon in zebrafish corresponds to the pallial brain regions in mammals, which form the cerebral cortex,[46,47] suggesting that NRCAM plays a conserved role in neurodevelopment of the pallium. However, the pallium, and in particular the cortex, is massively expanded in mammals and especially in humans. This may explain why the *nrcama*$^{\Delta}$ mutant zebrafish display a relatively modest phenotype compared to those observed in NRCAM-deficient individuals or may reflect the phenotypic variability observed among the affected individuals.

It is well established that neural adhesion molecules, including NRCAM, play a pivotal role in directing proper neurite outgrowth, axon guidance and pathfinding through the regions where they are expressed.[30,48,49] Indeed, previous *in vitro* studies of murine *Nrcam*-deficient cells revealed abnormal neurite outgrowth, as the cerebellar granule cells failed to extend neurites on substrates such as contactin-1.[34] Additional studies have shown that Nrcam is also required for synaptogenesis and interaction between Schwann cells and axons.[30,34,50] Nrcam has also been proven integral for formation and maintenance of nodes of Ranvier on myelinated axons, and peripheral nerves of Nrcam-deficient mice exhibit delayed or abnormal node formation.[30,49–51] In agreement with the above observations, we show that loss of *nrcama* function results in mildly altered axonal projections and abnormally increased swimming behavior in zebrafish larvae (Figures 3A–3H). The observed diverse clinical manifestations of either neuropathy and hypotonia or spasticity in affected individuals may result from misrouting of nerve fibers. Interestingly, this variable neurological and neuromuscular phenotype is also observed in individuals with *NFASC* variants, and spastic paraparesis is observed in individuals with *L1CAM* mutations.[6–9] These phenotypic overlaps caused by variants in different L1-Ig-CAM family proteins support the findings described in individuals with NRCAM-related disorder.

Previous studies revealed that *Nrcam*-deficiency in mice leads to mistargeting of motor and somatosensory thalamic axons to the visual cortex. As such, knockout (KO) mice have abnormal visual-evoked potential (VEP) recordings, suggesting poor visual acuity.[30,52] Pattern VEP was abnormal in individual 1 (Figure S4), and eye examinations were abnormal in some of the other affected individuals. While *Nrcam* is expressed in the lens, and *Nrcam*-deficient mice develop cataracts as a result of disorganization of lens fibers, only two individuals in this study (individuals 3 and 8a) exhibited signs of cataract on examination; the young age of most individuals described should be noted, as cataract may develop over time. Similarly, the observed hearing abnormalities in three of the affected individuals can be inferred to NRCAM expression in the spiral ganglion neurons, cochlear efferent fibers, and cochlear sensory cells within the inner ear. Nrcam loss in mice leads to abnormalities in cochlear afferent and efferent fibers, which are most prominent during developmental stages but appear to recover after hearing onset, and these mice do not exhibit significant hearing defects.[53] This recovery observed in *Nrcam*-deficient mice may explain the partial penetrance of this feature in the individuals described

herein. Considering that some individuals exhibited persistent hearing impairment, unlike KO mice with normal auditory acuity, this observation highlights the role of NRCAM in neural hearing in humans and suggests that humans possibly lack some compensatory mechanisms for NRCAM disruption.

Overall, there is a wide range of phenotypic expression in individuals with different *NRCAM* variants; no single feature is observed in 100% of the affected individuals described here, although different neuromuscular abnormalities, e.g., neuropathy, hypotonia, or spasticity, are present in all individuals, and GDD/cognitive impairment with congenital onset are prominent features (Figure 1B). Phenotypic heterogeneity is observed among numerous neurodevelopmental and other disorders, including *NFASC*- and *L1CAM*-related diseases[6,8,9,54] and suggests variant-specific effects or other modifiers.[54] Therefore, *NRCAM*-related phenotypes may either be considered as a single heterogeneous disorder or as several separate syndromes similarly to *L1CAM*. Generally speaking, we suggest a genotype-phenotype correlation, where individuals harboring LoF *NRCAM* variants tend to have a more severe phenotype than those with missense variants. However, the nature and location of each missense variant and their resulting effect on protein expression and function may also affect the subsequent clinical manifestations. Additional individuals affected by this disorder and further studies on the clinical presentation and natural history of these individuals will aid in establishing clearer genotype-phenotype correlations.

While Nrcam deficiency causes major abnormalities *in vitro*, mice with bi-allelic *Nrcam* loss do not recapitulate the severity of the human phenotype,[34] which is further evidenced in the *nrcama*$^{\Delta}$ bi-allelic loss-of-function zebrafish model presented here. *Nrcam* KO mice have mild defects, such as a mildly reduced cerebellar size in certain regions, without organization defects. In addition, while KO mice have delayed nodes of Ranvier formation and subsequently delayed sodium channel clustering at nodes, they do not exhibit signs of a neuromuscular disorder.[30,50,51] This may be a result of compensatory function by the other L1-Ig-CAM proteins in mice and zebrafish or as yet undetermined differences in Nrcam protein function between species. For example, the KGE and RNRR motifs found in the human NRCAM third Fn-III domain repeat, which are important for integrin and furin recognition and binding, respectively, are poorly conserved in zebrafish Nrcam (HGD and QDYD, respectively), potentially highlighting differences between the zebrafish and human protein functions. Interestingly, the first generated *L1cam* KO mice also exhibited a mild phenotype, and only switching to a different genetic background produced the expected syndromic model.[55,56] Moreover, recent studies suggest that the phenotypic discrepancies observed between complete-gene KOs and other disruptions in the same gene are caused by compensation responses initiated by alleles prone to nonsense-mediated mRNA decay (NMD). Alleles undergoing NMD could trigger compensatory activation of other genes with similar sequence or function and thus affect the resulting phenotype.[57–59] Nevertheless, studies have shown clear links between *Nrcam* and other neuropathy- or myopathy-related genes, e.g., *Sh3tc2*, *Gars*, and *Lpin1*, whereby mouse double KOs or mutant models exhibit an exacerbated neuropathic phenotype, suggesting a synergistic effect.[60,61]

In summary, our findings reveal a neurodevelopmental disorder caused by bi-allelic variants in *NRCAM*. The affected individuals' phenotype, which is marked by various neurological findings including GDD/intellectual disability, hydrocephalus, hypotonia, peripheral neuropathy and/or spasticity, abnormal brain imaging, and ocular and hearing defects, is highly supported by the role of NRCAM in nervous system development, protein expression, *in vivo* zebrafish studies, and *in vitro* studies of deficient cells.

Data and code availability

The data supporting the findings of this study are available upon request. *NRCAM* variants have been deposited to the ClinVar database (accession numbers ClinVar: SCV002044485 to ClinVar: SCV002044496).

Supplemental information

Supplemental information can be found online at https://doi.org/10.1016/j.ajhg.2022.01.004.

Acknowledgments

The authors would like to thank the affected individuals and their families for participating in this study. We thank Dr. Orly Eshach Adiv and Dr. Tova Hershkovitz for following and treating individual 1 and Dr. Tamar Paperna for her consultation on this project. We also acknowledge the excellent technical assistance of Mrs. Els De Vriendt, who performed the segregation analysis in family 8. The authors thank Monash Micro Imaging (MMI) facility, Monash AquaCore facility, Monash University for technical imaging and animal husbandry support. This work was funded by NHMRC project grants GNT1145048 and GNT 1138870 (J.K.) and a grant from the Cerebral Palsy Alliance (J.K., F.K., M.F., M.C.K., and S.B.). The Australian Regenerative Medicine Institute (ARMI) is supported by grants from the State Government of Victoria and the Australian Government. Portions of this work were funded by the National Institutes of Health (1R01 NS106298 to M.C.K.). In addition, we acknowledge the financial support received from the Fund for Scientific Research-Flanders (FWO), grant G049217N (A.J.). Research reported for individual 3 was supported by the National Institutes of Health (NIH) Common Fund, through the Office of Strategic Coordination/Office of the NIH Director (U01HG007672 to V.S., Duke University). The full list of members of the Undiagnosed Diseases Network (UDN) appears in the supplemental materials. The content is solely the responsibility of the authors and does not necessarily represent the official views of the NIH.

Declaration of interests

C.G.-J. is a full-time employee of the Regeneron Genetics Center and receives stock options as part of compensation. All other authors have no conflicts to declare.

Received: May 30, 2021
Accepted: January 7, 2022
Published: February 1, 2022

Web resources

1000 Genomes Project, https://www.internationalgenome.org/
ClinVar, https://www.ncbi.nlm.nih.gov/clinvar/
Combined Annotation-Dependent Depletion (CADD), https://cadd.gs.washington.edu/
dbSNP, https://www.ncbi.nlm.nih.gov/snp/
Ensembl, https://www.ensembl.org/index.html
GeneMatcher, https://genematcher.org/
Genomicus, https://www.genomicus.bio.ens.psl.eu/genomicus-100.01/cgi-bin/search.pl
gnomAD database, https://gnomad.broadinstitute.org
Human Splicing Finder (HSF), https://www.genomnis.com/access-hsf
MutationTaster, https://www.mutationtaster.org/
OMIM, https://omim.org/
PolyPhen-2, http://genetics.bwh.harvard.edu/pph2/
ProSA-web server, https://prosa.services.came.sbg.ac.at/prosa.php
SIFT, https://sift.bii.a-star.edu.sg/
SWISS-MODEL server, https://swissmodel.expasy.org/
Uniprot, https://www.uniprot.org/
Zebrafish Information Network (ZFIN), http://zfin.org/

References

1. Samatov, T.R., Wicklein, D., and Tonevitsky, A.G. (2016). L1CAM: Cell adhesion and more. Prog. Histochem. Cytochem. *51*, 25–32.
2. Volkmer, H., Schreiber, J., and Rathjen, F.G. (2013). Regulation of adhesion by flexible ectodomains of IgCAMs. Neurochem. Res. *38*, 1092–1099.
3. Hortsch, M. (2000). Structural and functional evolution of the L1 family: are four adhesion molecules better than one? Mol. Cell. Neurosci. *15*, 1–10.
4. Colombo, F., and Meldolesi, J. (2015). L1-CAM and N-CAM: From Adhesion Proteins to Pharmacological Targets. Trends Pharmacol. Sci. *36*, 769–781.
5. Kahle, K.T., Kulkarni, A.V., Limbrick, D.D., Jr., and Warf, B.C. (2016). Hydrocephalus in children. Lancet *387*, 788–799.
6. Stumpel, C., and Vos, Y.J. (2015). L1 Syndrome (Seattle: University of Washington).
7. Anazi, S., Maddirevula, S., Salpietro, V., Asi, Y.T., Alsahli, S., Alhashem, A., Shamseldin, H.E., AlZahrani, F., Patel, N., Ibrahim, N., et al. (2017). Expanding the genetic heterogeneity of intellectual disability. Hum. Genet. *136*, 1419–1429.
8. Smigiel, R., Sherman, D.L., Rydzanicz, M., Walczak, A., Mikolajkow, D., Krolak-Olejnik, B., Kosińska, J., Gasperowicz, P., Biernacka, A., Stawinski, P., et al. (2018). Homozygous mutation in the Neurofascin gene affecting the glial isoform of Neurofascin causes severe neurodevelopment disorder with hypotonia, amimia and areflexia. Hum. Mol. Genet. *27*, 3669–3674.
9. Monfrini, E., Straniero, L., Bonato, S., Monzio Compagnoni, G., Bordoni, A., Dilena, R., Rinchetti, P., Silipigni, R., Ronchi, D., Corti, S., et al. (2019). Neurofascin (NFASC) gene mutation causes autosomal recessive ataxia with demyelinating neuropathy. Parkinsonism Relat. Disord. *63*, 66–72.
10. Sobreira, N., Schiettecatte, F., Valle, D., and Hamosh, A. (2015). GeneMatcher: a matching tool for connecting investigators with an interest in the same gene. Hum. Mutat. *36*, 928–930.
11. Hershkovitz, T., Kurolap, A., Gonzaga-Jauregui, C., Paperna, T., Mory, A., Wolf, S.E., Overton, J.D., Shuldiner, A.R., Saada, A., Mandel, H., Baris Feldman, H.; and Regeneron Genetics Center (2019). A novel TUFM homozygous variant in a child with mitochondrial cardiomyopathy expands the phenotype of combined oxidative phosphorylation deficiency 4. J. Hum. Genet. *64*, 589–595.
12. McMichael, G., Bainbridge, M.N., Haan, E., Corbett, M., Gardner, A., Thompson, S., van Bon, B.W.M., van Eyk, C.L., Broadbent, J., Reynolds, C., et al. (2015). Whole-exome sequencing points to considerable genetic heterogeneity of cerebral palsy. Mol. Psychiatry *20*, 176–182.
13. Kancheva, D., Atkinson, D., De Rijk, P., Zimon, M., Chamova, T., Mitev, V., Yaramis, A., Maria Fabrizi, G., Topaloglu, H., Tournev, I., et al. (2016). Novel mutations in genes causing hereditary spastic paraplegia and Charcot-Marie-Tooth neuropathy identified by an optimized protocol for homozygosity mapping based on whole-exome sequencing. Genet. Med. *18*, 600–607.
14. Ta-Shma, A., Zhang, K., Salimova, E., Zernecke, A., Sieiro-Mosti, D., Stegner, D., Furtado, M., Shaag, A., Perles, Z., Nieswandt, B., et al. (2017). Congenital valvular defects associated with deleterious mutations in the *PLD1* gene. J. Med. Genet. *54*, 278–286.
15. Desmet, F.-O., Hamroun, D., Lalande, M., Collod-Béroud, G., Claustres, M., and Béroud, C. (2009). Human Splicing Finder: an online bioinformatics tool to predict splicing signals. Nucleic Acids Res. *37*, e67.
16. Biasini, M., Bienert, S., Waterhouse, A., Arnold, K., Studer, G., Schmidt, T., Kiefer, F., Gallo Cassarino, T., Bertoni, M., Bordoli, L., and Schwede, T. (2014). SWISS-MODEL: modelling protein tertiary and quaternary structure using evolutionary information. Nucleic Acids Res. *42*, W252-8.
17. Wiederstein, M., and Sippl, M.J. (2007). ProSA-web: interactive web service for the recognition of errors in three-dimensional structures of proteins. Nucleic Acids Res. *35*, W407-10.
18. Baker, N.A., Sept, D., Joseph, S., Holst, M.J., and McCammon, J.A. (2001). Electrostatics of nanosystems: application to microtubules and the ribosome. Proc. Natl. Acad. Sci. USA *98*, 10037–10041.
19. Fernandez-Recio, J., Totrov, M., Skorodumov, C., and Abagyan, R. (2005). Optimal docking area: a new method for predicting protein-protein interaction sites. Proteins *58*, 134–143.
20. Hamimi, M., Khabooshan, M., Castillo, H.A., and Kaslin, J. (2019). Fluorescently labeled TracrRNA improves work flow and facilitates successful genome editing in zebrafish. Zebrafish *16*, 135–137.
21. Lindsey, B.W., Aitken, G.E., Tang, J.K., Khabooshan, M., Douek, A.M., Vandestadt, C., and Kaslin, J. (2019). Midbrain tectal stem cells display diverse regenerative capacities in zebrafish. Sci. Rep. *9*, 4420.

22. Kaslin, J., Ganz, J., Geffarth, M., Grandel, H., Hans, S., and Brand, M. (2009). Stem cells in the adult zebrafish cerebellum: initiation and maintenance of a novel stem cell niche. J. Neurosci. *29*, 6142–6153.
23. Kaslin, J., and Panula, P. (2001). Comparative anatomy of the histaminergic and other aminergic systems in zebrafish (Danio rerio). J. Comp. Neurol. *440*, 342–377.
24. Kurolap, A., Eshach-Adiv, O., Hershkovitz, T., Paperna, T., Mory, A., Oz-Levi, D., Zohar, Y., Mandel, H., Chezar, J., Azoulay, D., et al. (2017). Loss of CD55 in Eculizumab-Responsive Protein-Losing Enteropathy. N. Engl. J. Med. *377*, 87–89.
25. Kurolap, A., Eshach Adiv, O., Hershkovitz, T., Tabib, A., Karbian, N., Paperna, T., Mory, A., Vachyan, A., Slijper, N., Steinberg, R., et al. (2019). Eculizumab Is Safe and Effective as a Long-term Treatment for Protein-losing Enteropathy Due to CD55 Deficiency. J. Pediatr. Gastroenterol. Nutr. *68*, 325–333.
26. Cirstea, I.C., Gremer, L., Dvorsky, R., Zhang, S.C., Piekorz, R.P., Zenker, M., and Ahmadian, M.R. (2013). Diverging gain-of-function mechanisms of two novel KRAS mutations associated with Noonan and cardio-facio-cutaneous syndromes. Hum. Mol. Genet. *22*, 262–270.
27. Cool, R.H., Schmidt, G., Lenzen, C.U., Prinz, H., Vogt, D., and Wittinghofer, A. (1999). The Ras mutant D119N is both dominant negative and activated. Mol. Cell. Biol. *19*, 6297–6305.
28. Fu, X.D. (1993). Specific commitment of different pre-mRNAs to splicing by single SR proteins. Nature *365*, 82–85.
29. Ishiguro, H., Liu, Q.-R., Gong, J.-P., Hall, F.S., Ujike, H., Morales, M., Sakurai, T., Grumet, M., and Uhl, G.R. (2006). NrCAM in addiction vulnerability: positional cloning, drug-regulation, haplotype-specific expression, and altered drug reward in knockout mice. Neuropsychopharmacology *31*, 572–584.
30. Sakurai, T. (2012). The role of NrCAM in neural development and disorders–beyond a simple glue in the brain. Mol. Cell. Neurosci. *49*, 351–363.
31. Leahy, D.J., Aukhil, I., and Erickson, H.P. (1996). 2.0 A crystal structure of a four-domain segment of human fibronectin encompassing the RGD loop and synergy region. Cell *84*, 155–164.
32. Simões, I., Mueller, E.C., Otto, A., Bur, D., Cheung, A.Y., Faro, C., and Pires, E. (2005). Molecular analysis of the interaction between cardosin A and phospholipase D(α). Identification of RGD/KGE sequences as binding motifs for C2 domains. FEBS J. *272*, 5786–5798.
33. Randlett, O., Wee, C.L., Naumann, E.A., Nnaemeka, O., Schoppik, D., Fitzgerald, J.E., Portugues, R., Lacoste, A.M., Riegler, C., Engert, F., and Schier, A.F. (2015). Whole-brain activity mapping onto a zebrafish brain atlas. Nat. Methods *12*, 1039–1046.
34. Sakurai, T., Lustig, M., Babiarz, J., Furley, A.J.W., Tait, S., Brophy, P.J., Brown, S.A., Brown, L.Y., Mason, C.A., and Grumet, M. (2001). Overlapping functions of the cell adhesion molecules Nr-CAM and L1 in cerebellar granule cell development. J. Cell Biol. *154*, 1259–1273.
35. Lustig, M., Erskine, L., Mason, C.A., Grumet, M., and Sakurai, T. (2001). Nr-CAM expression in the developing mouse nervous system: ventral midline structures, specific fiber tracts, and neuropilar regions. J. Comp. Neurol. *434*, 13–28.
36. Brand, Y., Sung, M., Pak, K., Chavez, E., Wei, E., Radojevic, V., Bodmer, D., and Ryan, A.F. (2015). Neural cell adhesion molecule NrCAM is expressed in the mammalian inner ear and modulates spiral ganglion neurite outgrowth in an in vitro alternate choice assay. J. Mol. Neurosci. *55*, 836–844.
37. Matzel, L.D., Babiarz, J., Townsend, D.A., Grossman, H.C., and Grumet, M. (2008). Neuronal cell adhesion molecule deletion induces a cognitive and behavioral phenotype reflective of impulsivity. Genes Brain Behav. *7*, 470–480.
38. Ishiguro, H., Miyake, K., Tabata, K., Mochizuki, C., Sakurai, T., and Onaivi, E.S. (2019). Neuronal cell adhesion molecule regulating neural systems underlying addiction. Neuropsychopharmacol Rep. *39*, 10–16.
39. Ogungbemi, A., Leuthold, D., Scholz, S., and Küster, E. (2019). Hypo- or hyperactivity of zebrafish embryos provoked by neuroactive substances: a review on how experimental parameters impact the predictability of behavior changes. Environ. Sci. Eur. *31*, 88.
40. Basnet, R.M., Zizioli, D., Taweedet, S., Finazzi, D., and Memo, M. (2019). Zebrafish larvae as a behavioral model in neuropharmacology. Biomedicines *7*, 23.
41. Bai, Y., Liu, H., Huang, B., Wagle, M., and Guo, S. (2016). Identification of environmental stressors and validation of light preference as a measure of anxiety in larval zebrafish. BMC Neurosci. *17*, 63.
42. Barclay, A.N. (2003). Membrane proteins with immunoglobulin-like domains–a master superfamily of interaction molecules. Semin. Immunol. *15*, 215–223.
43. Chi-Rosso, G., Gotwals, P.J., Yang, J., Ling, L., Jiang, K., Chao, B., Baker, D.P., Burkly, L.C., Fawell, S.E., and Koteliansky, V.E. (1997). Fibronectin type III repeats mediate RGD-independent adhesion and signaling through activated β1 integrins. J. Biol. Chem. *272*, 31447–31452.
44. Matsuda, K., Yoshida, M., Kawakami, K., Hibi, M., and Shimizu, T. (2017). Granule cells control recovery from classical conditioned fear responses in the zebrafish cerebellum. Sci. Rep. *7*, 11865.
45. Lal, P., Tanabe, H., Suster, M.L., Ailani, D., Kotani, Y., Muto, A., Itoh, M., Iwasaki, M., Wada, H., Yaksi, E., and Kawakami, K. (2018). Identification of a neuronal population in the telencephalon essential for fear conditioning in zebrafish. BMC Biol. *16*, 45.
46. Jan, K., and Ganz, J. (2020). Zebrafish Nervous Systems. In The Zebrafish in Biomedical Research, S.C. Cartner, J.S. Eisen, S.C. Farmer, K.J. Guillemin, M.L. Kent, and G.E. Sanders, eds. (Academic Press, Elsevier), pp. 181–189.
47. Kaslin, J., and Brand, M. (2013). Cerebellar Development and Neurogenesis in Zebrafish. In Handbook of the Cerebellum and Cerebellar Disorders, M. Manto, D. Gruol, J. Schmahmann, N. Koibuchi, and F. Rossi, eds. (Springer), pp. 1441–1462.
48. Tessier-Lavigne, M., and Goodman, C.S. (1996). The Molecular Biology of Axon Guidance. Science *274*, 1123–1133.
49. Sakisaka, T., and Takai, Y. (2005). Cell adhesion molecules in the CNS. J. Cell Sci. *118*, 5407–5410.
50. Amor, V., Feinberg, K., Eshed-Eisenbach, Y., Vainshtein, A., Frechter, S., Grumet, M., Rosenbluth, J., and Peles, E. (2014). Long-term maintenance of Na+ channels at nodes of Ranvier depends on glial contact mediated by gliomedin and NrCAM. J. Neurosci. *34*, 5089–5098.
51. Custer, A.W., Kazarinova-Noyes, K., Sakurai, T., Xu, X., Simon, W., Grumet, M., and Shrager, P. (2003). The role of the ankyrin-binding protein NrCAM in node of Ranvier formation. J. Neurosci. *23*, 10032–10039.

52. Demyanenko, G.P., Riday, T.T., Tran, T.S., Dalal, J., Darnell, E.P., Brennaman, L.H., Sakurai, T., Grumet, M., Philpot, B.D., and Maness, P.F. (2011). NrCAM deletion causes topographic mistargeting of thalamocortical axons to the visual cortex and disrupts visual acuity. J. Neurosci. *31*, 1545–1558.
53. Harley, R.J., Murdy, J.P., Wang, Z., Kelly, M.C., Ropp, T.F., Park, S.H., Maness, P.F., Manis, P.B., and Coate, T.M. (2018). Neuronal cell adhesion molecule (NrCAM) is expressed by sensory cells in the cochlea and is necessary for proper cochlear innervation and sensory domain patterning during development. Dev. Dyn. *247*, 934–950.
54. Pizzo, L., Jensen, M., Polyak, A., Rosenfeld, J.A., Mannik, K., Krishnan, A., McCready, E., Pichon, O., Le Caignec, C., Van Dijck, A., et al. (2019). Rare variants in the genetic background modulate cognitive and developmental phenotypes in individuals carrying disease-associated variants. Genet. Med. *21*, 816–825.
55. Patzke, C., Acuna, C., Giam, L.R., Wernig, M., and Südhof, T.C. (2016). Conditional deletion of L1CAM in human neurons impairs both axonal and dendritic arborization and action potential generation. J. Exp. Med. *213*, 499–515.
56. Tapanes-Castillo, A., Weaver, E.J., Smith, R.P., Kamei, Y., Caspary, T., Hamilton-Nelson, K.L., Slifer, S.H., Martin, E.R., Bixby, J.L., and Lemmon, V.P. (2010). A modifier locus on chromosome 5 contributes to L1 cell adhesion molecule X-linked hydrocephalus in mice. Neurogenetics *11*, 53–71.
57. Sherry, S.T., Ward, M.H., Kholodov, M., Baker, J., Phan, L., Smigielski, E.M., and Sirotkin, K. (2001). dbSNP: the NCBI database of genetic variation. Nucleic Acids Res. *29*, 308–311.
58. Ma, Z., Zhu, P., Shi, H., Guo, L., Zhang, Q., Chen, Y., Chen, S., Zhang, Z., Peng, J., and Chen, J. (2019). PTC-bearing mRNA elicits a genetic compensation response via Upf3a and COMPASS components. Nature *568*, 259–263.
59. El-Brolosy, M.A., Kontarakis, Z., Rossi, A., Kuenne, C., Günther, S., Fukuda, N., Kikhi, K., Boezio, G.L.M., Takacs, C.M., Lai, S.L., et al. (2019). Genetic compensation triggered by mutant mRNA degradation. Nature *568*, 193–197.
60. Morelli, K.H., Seburn, K.L., Schroeder, D.G., Spaulding, E.L., Dionne, L.A., Cox, G.A., and Burgess, R.W. (2017). Severity of Demyelinating and Axonal Neuropathy Mouse Models Is Modified by Genes Affecting Structure and Function of Peripheral Nodes. Cell Rep. *18*, 3178–3191.
61. Douglas, D.S., Moran, J.L., Bermingham, J.R., Jr., Chen, X.-J., Brindley, D.N., Soliven, B., Beier, D.R., and Popko, B. (2009). Concurrent Lpin1 and Nrcam mouse mutations result in severe peripheral neuropathy with transitory hindlimb paralysis. J. Neurosci. *29*, 12089–12100.